FIRST QUARTERLY PROGRESS REPORT

INVESTIGATION OF CURRENT

DEGRADATION PHENOMENON

IN SUPERCONDUCTING SOLENOIDS

Contract NAS 8-5356

July 15, 1964 to October 15, 1964

L. C. Salter, Jr.

ATOMICS INTERNATIONAL

A DIVISION OF NORTH AMERICAN AVIATION, INC.
P.O. BOX 309   CANOGA PARK, CALIFORNIA

FIRST QUARTERLY PROGRESS REPORT

INVESTIGATION OF CURRENT DEGRADATION PHENOMENON

IN SUPERCONDUCTING SOLENOIDS

July 15, 1964 to October 15, 1964

Contract No. NAS 8-5356

ABSTRACT

13285

A one-turn loop of 0.010" dia Nb-25% Zr wire has been
tested in time-varying transverse magnetic fields in an
attempt to see rapid or catistrophic flux penetration. A
one-turn Cu search-coil was used to monitor the field. Flux
perturbations were seen but were finally attributed to
localized flux changes in the superconducting solenoid used
to supply the external field.

In a second experiment, the multi-probe solenoid was
driven normal in external fields between 0 and 18.7 kG.
The location of the normal region moved progressively from
the high-field inner windings of the multi-probe coil to
the geometrical ends of the coil as the external field
ranged from zero to maximum.

Several 0.010" dia Ti-22 [a]/o wires were drawn and heat-
treated to provide a variety in metallurigical structure and
critical currents. Twenty of 30 samples have been heat-
treated and seven of these have been subjected to metallography
and critical current density versus transverse field tests.

author

1

I. SUPERCONDUCTING WIRE LOOP

A. Description

The object of this experiment was to search for rapid or catostrophic flux penetration into a one-turn loop of Nb-25% Zr wire. The loop and search coils were orientated perpendicular to a time-varying magnetic field and secured with a Teflon holder as shown in Figure 1a. The mounting and circuitry (Figure 1b) are discussed below.

One search coil (SC-1) and the Nb-Zr wire are held in close proximity with a V groove in the Teflon holder. A second search coil (SC-2), which is removed 0.2" from the Nb-Zr loop, is used to monitor background noise and check for coincidences between flux jumps in the Nb-Zr loop, seen by SC-1, and the external superconducting solenoid. The ends of the Nb-Zr loop bend 90° and pass along the Teflon rod, parallel to the field, to the low-field region where a superconducting pressure joint is made. Voltage probes are attached to the Nb-Zr leads as shown. The various wires are secured with adhesive Mylar tape and the apparatus is inserted in a 0.75" i.d. superconducting solenoid. The Nb-Zr wire is secured between the machined V groove and the magnet coil form with a snug fit.

The two search-coils and the Nb-Zr loop voltage probes are monitored with a Tektronix Type 555 oscilloscope in conjunction with either a Tektronix Type E, high-gain plug-in unit, or a Tektronix Type 1121 pre-amplifier powering a Type L plug-in unit. The Type E plug-in has a sensitivity of 50 μV/cm but is limited in its frequency response, at this sensitivity, to 20-60 kC. The 1121 preamplifier and Type L arrangement has 15 nanosec rise-time and a sensitivity limited by the 50 uV rms noise level of the 1121 preamplifier.

The superconducting solenoid, rated at 5.00 kG/A with a maximum field of 49 kG, is powered by an electronically controlled, regulated dc power supply. This controlled supply can deliver up to 100 A at ramp rates of 0.001 A/sec to 10 A/sec with a current ripple less than 10 mA.

2

B.   Experiments

Three separate experiments were run. In the first experiment, the superconducting loop was closed and would sustain induced persistent transport currents. The external field was increased at a rate of 200 gauss/sec. At approximately 500 gauss intervals, the loop would go normal. A typical pulse seen by the pick-up loop SC-1 is shown in Figure 2a. The trapped flux is the area under this voltage trace and equals 70 maxwells. The coupling coefficient between the Nb-Zr loop and SC-1 is calculated to be ~0.7, assuming a 0.004" gap between the two wires (0.001" insulation on each wire and an estimated 0.002" gap due to positioning errors). Thus, the Nb-Zr loop shielded ~$\frac{70}{0.7}$ = 100 maxwells. From an IBM 7094 calculation, the flux due to a transport current in the test loop is φ = 5.6 maxwells/A. Thus, the current in the Nb-Zr loop is $\frac{100}{5.6}$ = 18 A. This value is consistent with previous findings[1] which showed that the $\frac{dH}{dt}$ induced, super-current instabilities in this wire (unstable Type A) began at ~ 20A. Therefore, the results of this one-turn solenoid simulation are consistent with the short-wire instability tests.

The trapped flux of ~ 100 maxwells is equivalent to an external field change of 280 gauss. Since SN transitions occurred for an external field change of 500 gauss, the remaining 220 gauss could result from continual field penetration while the sample is recovering from the SN transition.

It is doubtful that the loss of flux is due to flux creep as described by Kim, Hempstead, and Strnad [2,3] because such unstable wires do not appear to permit observable flux creep during our laboratory time scale.

In the second experiment, the superconducting loop is open circuited. In this configuration, no transport current can exist in the loop, and any perturbation in the magnetic field adjacent to the wire must be due to magnetization currents in the Nb-Zr loop. If these currents reach saturation, flux penetration into the wire can occur and pulses might be seen in SC-1.

3

The external field was again swept and pulses like the one recorded in Figure 2b were seen from SC-1. The upper trace was recorded using the Type E plug-in while the lower trace was recorded using the Tectronix 1121 wide-band amplifier. The lower trace is a factor of 10 faster and shows no additional character other than noise. The flux change registered is approximately 0.1 maxwells.

Coincidence observations between SC-1 and the voltage probes across the superconducting loop, see Figure 3a, show that both wires see a net flux change and that this change was greater in the Nb-Zr loop. SC-2 was also monitored, and pulses similar to those seen from SC-1 were found but did not coincide with the SC-1 events. It appears that the pulses originated in the super-magnet but were localized.

In a third experiment, conducted to confirm the origin of these pulses, the Nb-Zr loop was replaced with a 0.010" dia copper wire. The preceeding experiment was repeated and the pulses shown in Figure 3b were observed from the 0.010" dia copper wire loop. The lowest voltage trace is noise, the intermediate trace shows typical small pulses, and the largest pulse, though partially blanked by the scope, is essentially the same as seen in the Nb-Zr loop in Figure 3a. The largest pulses were observed in the same field range (10-20 kG), as those seen from search coils and the Nb-Zr loop (Figures 2b-3a). Thus, the pulses observed in the second experiment originated in the windings of the super-magnet immediately adjacent to the Nb-Zr loop

C.   Conclusions

Several conclusions can be drawn from these experiments. First, critical currents in one-turn, superconducting loops parallel solenoid and short sample current behavior quite closely in that the loop critical current is essentially the same as solenoid critical currents ($\sim$ 18A) and also the same as the maximum stable super-current found in short sample tests of the same wire. Second, flux jumps could not be detected in this single turn solenoid simulation with the single loop search coils. Third, a superconducting solenoid can be a noisy source in transient magnet field work. However, super-magnets should be very quiet for constant field work, especially if persistent switches are employed.

4

II. MULTI-PROBE SOLENOID STUDIES

A. Tests in External Fields

The multi-probe solenoid has been tested in external fields up to 18.7 kG. The external fields, supplied by a 7 cm i.d., 20 cm long superconducting solenoid, were homogeneous to $\pm$ 10% over the volume of the multi-probe solenoid. During all tests, the external field, H_e, was held constant, while the self-field of multi-probe magnet, H_m, was increased at a constant rate of 100 gauss/sec until an SN transition occurred. The normal region was then mapped using the magnet core sensing array described in previous reports. In all tests, H_e and H_m were in the same direction and were the central fields of the respective solenoid.

Figure 4 is a picture of the multi-probe solenoid, solenoid support, and magnetic core sensing array. Figures 5a-f are cross-sectional views of the multi-probe windings and show the location and shape of the normal region after each transition. Examination of these figures reveals the following pattern. The normal region is located near one end of the solenoid when H_e = 20 kG (Figures 5a-c). At lower values of H_e (Figure 5a), the normal region is concentrated in the coil, but includes part of the central, inner windings. At still lower fields (Figure 5e), the shape of the normal region approaches that for no external field, in which the ends of the coil remain superconducting. The normal regions in Figures 5a, b, and c are relatively small, possibly because there is less magnetic energy to propagate the normal region than in the subsequent tests.

When the multi-probe experienced an SN transition, the external solenoid would go normal also, and it is not known which coil was the initiator. This question is to be resolved. No matter which coil initiated the transitions, an important result is that the transition was transferred to the second coil electromagnetically instead of thermally because, in every transition the multi-probe windings between the external solenoid and the normal regions in the multi-probe coil remain superconducting.

5

B. Tests of Magneto-Resistance Probes

Non-inductively wound, copper-wire, magneto-resistance probes have been constructed and tested for sensitivity in fields up to 15 kG. A sensitivity of 2 gauss or ~0.01% has been achieved. In the event that extended multi-probe studies appear informative, local fields can be monitored with the above probes imbedded in the windings.

III. Ti-Nb CHARACTERIZATION

The metallurgical portion of this program is designed to produce variations in the superconducting properties (in particular, short sample and magnet critical currents, magnetization, and upper critical field) of the selected Ti-Nb alloy through metallurgical treatment; specifically variations in defects and defect density by heat treatment. Ultimately, superconducting properties will be compared with metallurgical structure in an attempt to understand how to construct better superconductor magnet material. Effort during the report period was in cold-drawing the swaged 0.025" dia Ti-22 a/o Nb wire to 0.010" dia, post-draw annealing samples of the wire, and evaluation of some of the metallurgical and superconducting properties of the samples.

Prior to drawing, the swaged 0.025" dia wire was stress-relieved at 550°C for 4 hours. For this anneal, the wire was encapsulated under a dynamic vacuum of $<10^{-5}$ mm Hg in an outgassed quartz combustion tube that was packed with a Zr getter. The annealed wire was quenched by rupturing the quartz tube under quenching oil. Attempts to cold-draw the annealed 0.025" wire with conventional drawing techniques and die lubricants were unsuccessful. We subsequently found that anodizing the wire rendered it drawable. The wire could then be reduced 5-10% (0.001") per drawing pass to the 0.010" diameter. Some difficulty was experienced during the initial few passes (down to 0.020"), but this was attributed to the poor surface condition of the as-swaged wire. The thickness of the anodized layer was not critical. The anodizing treatment used a saturated oxalic acid solution with a stainless steel cathode. Although the anodized layer could be formed with potentials between 5 and 75 V, 22 to 25 V were found to provide the most adherent film and, therefore, the best drawing lubricant.

Half of the wire was given an intermediate 800°C anneal at 0.016" dia. Although this rendered the material more ductile, the wire work-hardened more rapidly and displayed a greater tendency to seize in the die and break at high drawing speeds than did the 550°C annealed wire.

7

The reason for this is not readily apparent since the higher temperature anneal supposedly results in a single-phase material. A degree of matrix contamination with intersititial impurities of oxygen, nitrogen or hydrogen and the resultant formation of a second phase may be the cause of this anomalous behavior.

Heat treatments of the 0.010" dia wire are in progress according to the statistically-based schedule shown in Figure 6. Two 4" long samples are annealed at each time and temperature. One sample is for metallurgical examinations and magnetization and T_c tests. The second sample is bent before anneal into hair-pin shape for the J_c versus transverse H tests. The first twenty samples have been annealed. Pre- and post-anneal room-temperature resistivities have been determined for most of these twenty samples as well as for the as-drawn 550°C and 800°C wire. These data are tabulated in Table I. Metallography has also been completed on samples 1-7 and the as-drawn wire. Typical microstructures are shown in Figures 7-16.

Critical currents as a function of transverse applied fields have also been measured for samples 1-7 and the as-drawn wires. The results are presented in Figure 17. Although sufficient data are not yet available to firmly fix the dependence of J_c on annealing time and temperature, the present results are very encouraging since the critical current capacity of this material is responsive to both time and temperature variations.

A solenoid for use in the magnetization measurements of the Ti-Nb wires is under construction. A moving search-coil arrangement is also being constructed for measuring the magnetization of the 0.010" dia wire samples. The sensitivity of this arrangement will be about 10^{-3} maxwells.

8

IV. SUMMARY AND FUTURE PLANS

The investigation of flux jumping in individual wires and of SN transitions in solenoids has been unrevealing. The former experiment showed that flux jumps could not be detected in an open one-turn, Nb-Zr loop. The later experiment showed that, although the SN transitions can be followed and mapped, further interpretations of the results were virtually impossible. Although both of these approaches suggest additional experiments, we feel that other work should have higher priority.

On the other hand, the response of the Ti-Nb to the warm-aging treatments has been very encouraging. The critical current of the wire is quite sensitive to both time and temperature variations. Thus, it appears more constructive to fully characterize this material and lay a sounder basis for any future multi-probe work.

The metallurgical characterization includes a study of at least 30 wire samples, where 18 had been planned. Other measurements include both longitudinal and transverse field magnetization as well as T_c and H_{c2} measurements. The effect of copper-plating on the wire in small magnets will also be checked.

During the next quarter we will concentrate on completing the wire sampling. Photomicrographs, x-ray diffraction and electron beam studies will be completed as will the analyses of matrix and precipitate composition, and precipitate size and density. Measurements of magnetization and T_c will have been set up and tests should be completed. Attempts will be made to correlate the metallurgical structure with critical-current models as determined by the J_c versus H and magnetization measurements.

REFERENCES

1. Salter, L. C., "Investigation of Current Degradation Phenomenon In Superconducting Solenoids," AI-64-198, May 1964.

2. Kim, Y. B., Hampstead, C. F., and Strnad, A. R., Phys. Rev. Letters 9, 306 (1962).

3. Kim, Y. B., Hampstead, C. F., and Strnad, A. R., Phys. Rev. 129, 528 (1963).

TABLE I

Sample	Annealing Parameters Time (Minutes)	Temp. (°C)	As-Drawn Resistivity ρ_o (ohm-cm)$\cdot 10^6$	Post-Anneal Resistivity ρ_f (ohm-cm)$\cdot 10^6$	ρ_f/ρ_o	Hardness (KHN)	Critical Current Density J_c @ 30kG (amp/cm^2)$\cdot 10^{-4}$
1	3000	650	117	108	.92	216	< 0.85
2	10	200	110	107	.97	241	Bad Joint
3	3000	250	116	88	.76	480	6.00
4	1000	250	117	105	.90	426	3.01
5	10	600	115	85	.74	226	1.92
6	300	600	113	88	.78	236	< 0.85
7	100	500	117	72	.61	211	7.71
8	3000	550	121	77	.64		
9	300	500	119	71	.60		
10	3000	200	117	107	.91		
11	30	650	115	113	.99		
12	1000	600	115	90	.78		
13	1000	300	116	82	.71		
14	1000	350	113	68	.60		
15	3000	300	(data not available at this writing)				
16	1000	550	(data not available at this writing)				
17	100	350	112	75	.67		
18	10	250	116	103	.89		
19	100	900	113	71	.62		
20	30	550	112	77	.68		
550*	$\sim \infty$	20	74	-	-	260	3.10
800*	$\sim \infty$	20	113	-	-	282	5.00

*These sample designations were chosen to represent the as-drawn or cold-worked state for material annealed at 550°C and 800°C prior to reduction to 0.010" mil wire
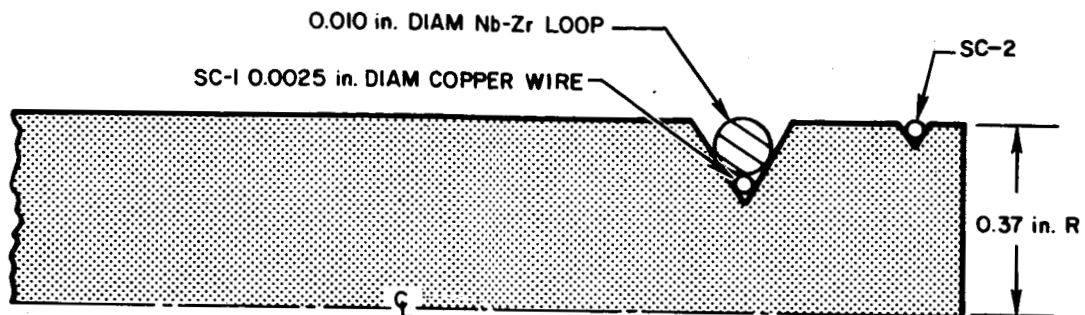
11

0.010 in. DIAM Nb-Zr LOOP

SC-I 0.0025 in. DIAM COPPER WIRE

SC-2

0.37 in. R

Figure la. Cross-section of Nb-Zr Loop and Copper Search Loops
Mounted on Teflon Holder.

90° BEND INTO PAGE

H(APPLIED)

COAXIAL CABLE TO SCOPE

$\otimes$ H(APPLIED)

SUPERCONDUCTING JOINT
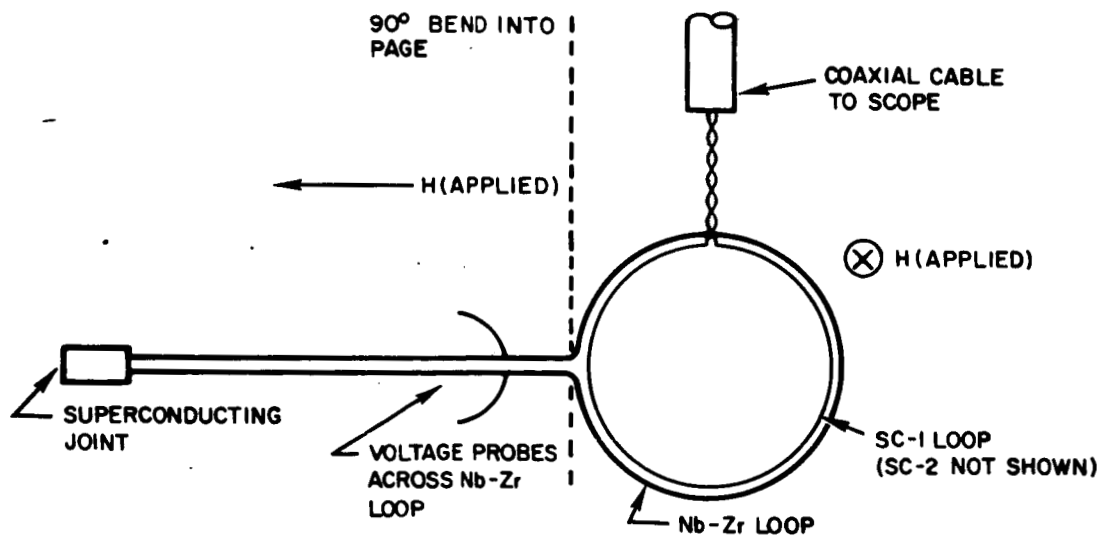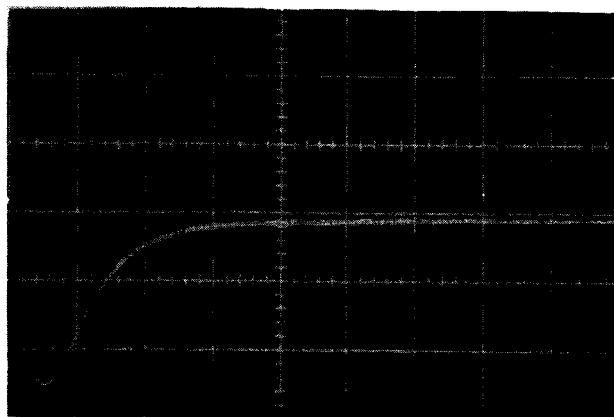
VOLTAGE PROBES ACROSS Nb-Zr LOOP

SC-I LOOP (SC-2 NOT SHOWN)

Nb-Zr LOOP

Figure lb. Circuitry for Nb-Zr and Search-Coil Loops.

5 mV/Cm

H = 15 kG

$$\frac{dH}{dt} = 500 \text{ gauss/sec}$$

. 50 μS/Cm

Figure 2a.   Pulse from SC-1 With Nb-Zr Loop in the Persistent Mode.

50 μV/Cm

upper trace: 10 μS/Cm
lower trace: 1 μS/Cm
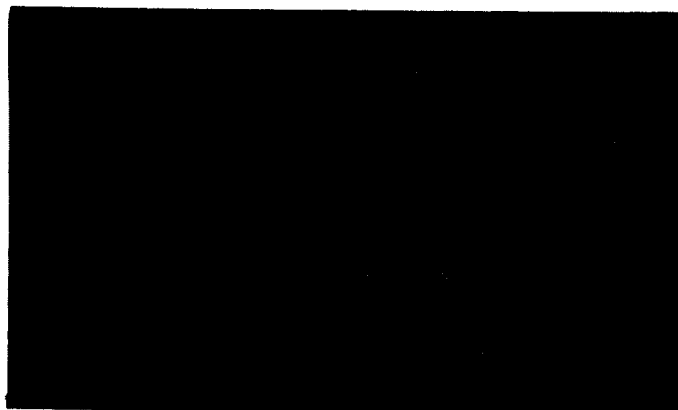
<u>Amplifier</u>

Type E Plug-in

Tektronic 1121
with Type L Plug-in

H = 15 kG

$$\frac{dH}{dt} = 500 \text{ gauss/sec}$$

Figure 2b.   Pulse from SC-1 with Nb-Zr Loop Open Circuited.

13

50 μV/Cm
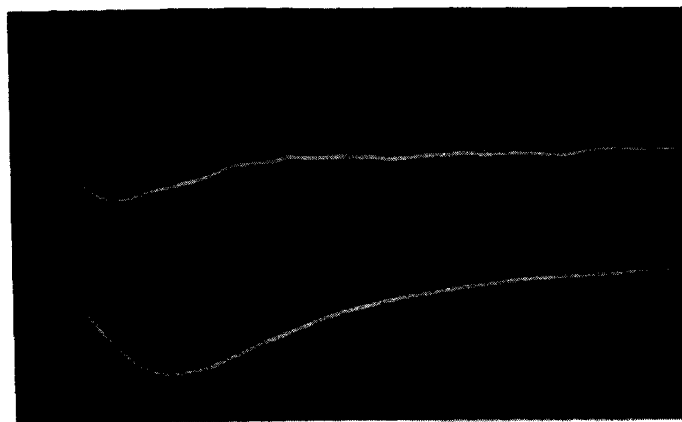
SC-1

Nb-Zr loop

H = 15 kG

$\frac{dH}{dt}$ = 500 gauss/sec

10 μS/Cm

Figure 3a.   Simultaneous Traces from SC-1 and Nb-Zr Loop

50 μV/Cm

H = 15 kG

$\frac{dH}{dt}$ = 500 gauss/sec

10 μS/Cm

Figure 3b.   Pulse from 0.010" dia Copper Wire Loop Substituting for the
Nb-Zr Loop.
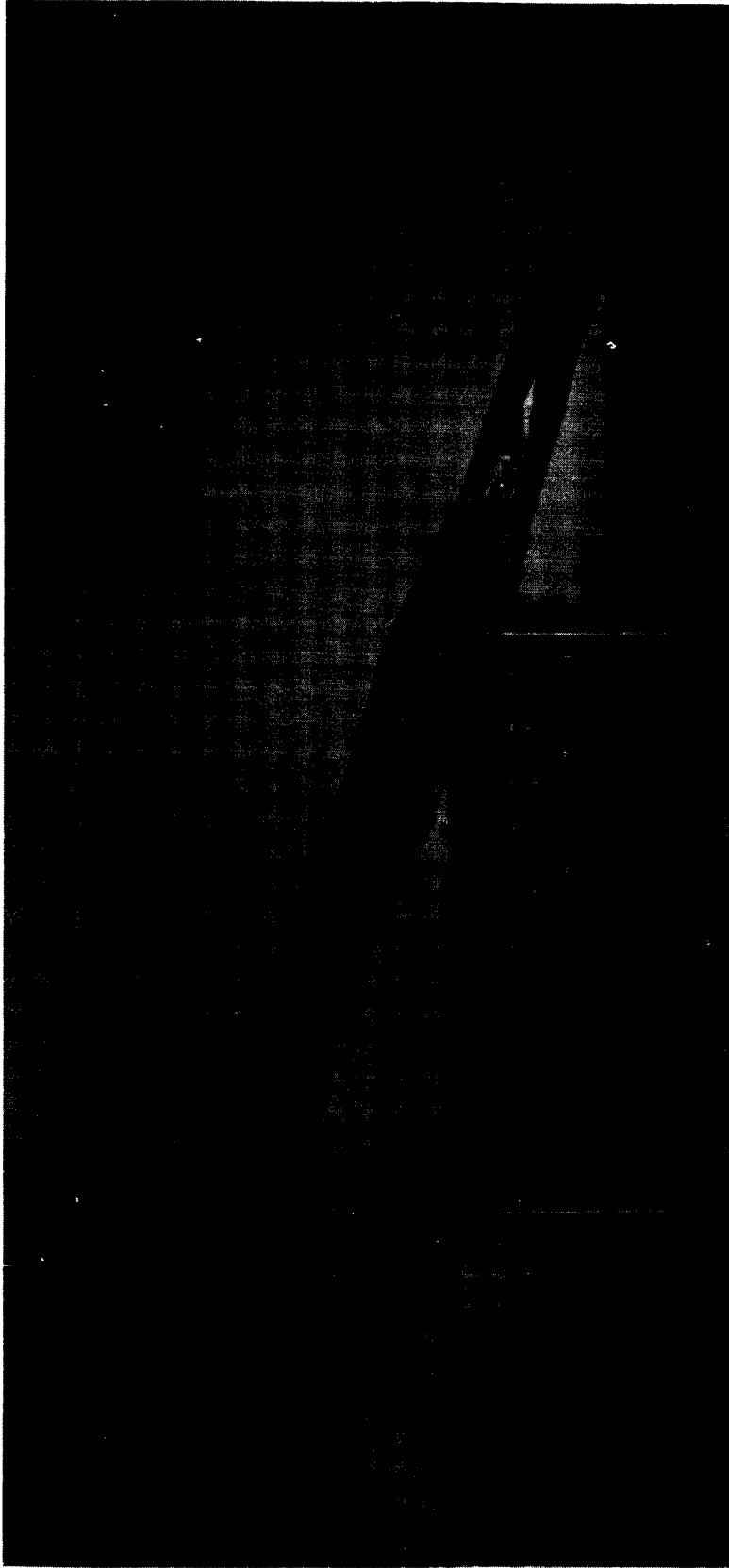
OO-101329

Figure 4. Photograph of Multi-probe Solenoid Showing Solenoid and Support Structure and 85 Pairs of Voltage Probes leading from the Solenoid to the Magnetic-core Sensing Array.

A voltage across a probe of 0.1 volt-sec or more will Reverse the Magnetization of the Magnetic Cores. Pressing the appropriate push-button switch on the face of the array, resets the core and a voltage is generated in the core secondary windings and read on a VTVM.
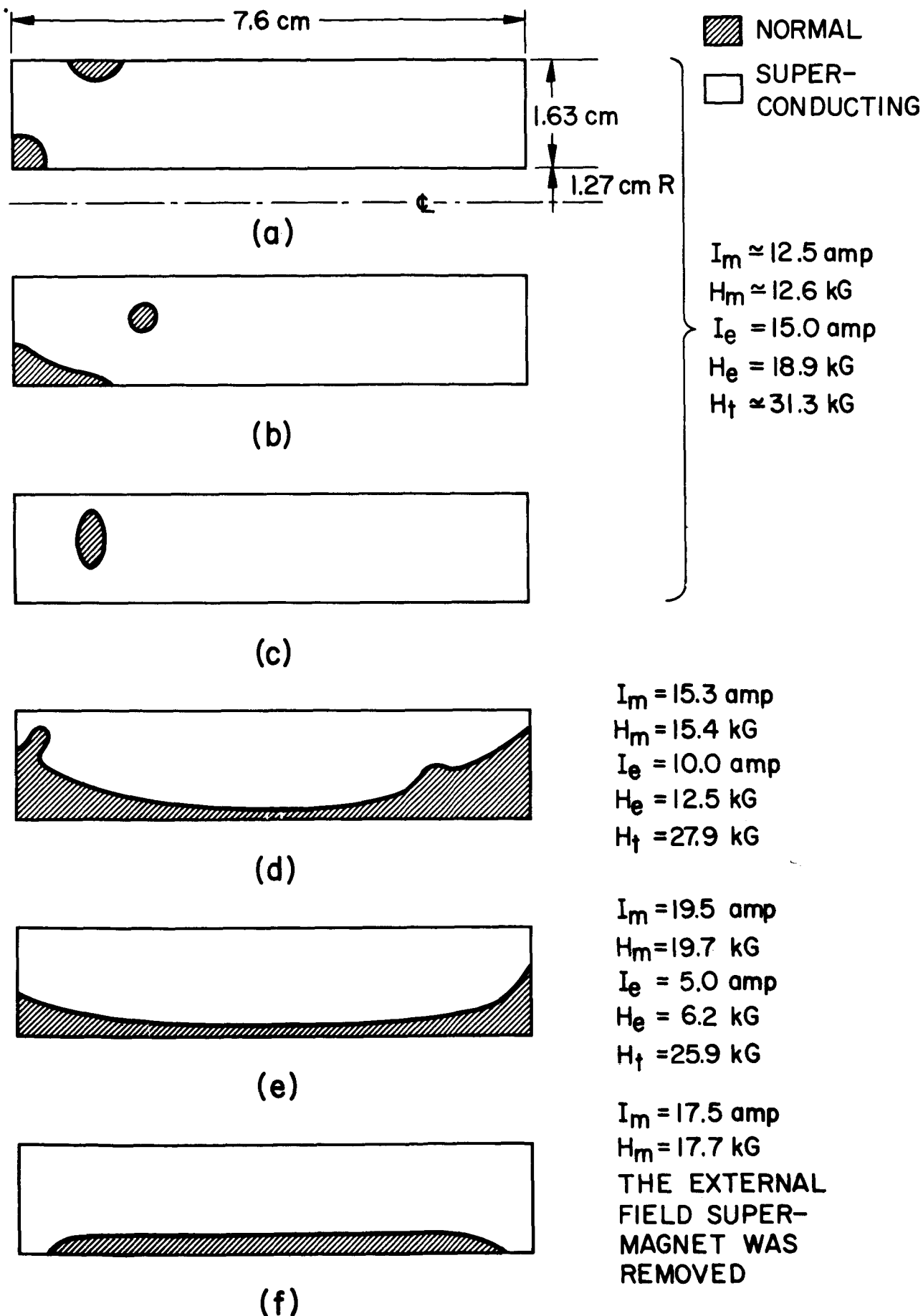
NORMAL

SUPER-
CONDUCTING

7.6 cm

1.63 cm

1.27 cm R

(a)

(b)

(c)

$I_m \simeq 12.5$ amp

$H_m \simeq 12.6$ kG

$I_e = 15.0$ amp

$H_e = 18.9$ kG

$H_t \simeq 31.3$ kG

(d)

$I_m = 15.3$ amp

$H_m = 15.4$ kG

$I_e = 10.0$ amp

$H_e = 12.5$ kG

$H_t = 27.9$ kG

(e)

$I_m = 19.5$ amp

$H_m = 19.7$ kG

$I_e = 5.0$ amp

$H_e = 6.2$ kG

$H_t = 25.9$ kG

(f)

$I_m = 17.5$ amp

$H_m = 17.7$ kG

THE EXTERNAL
FIELD SUPER-
MAGNET WAS
REMOVED

Figure 5   Multi-probe Solenoid Cross Section Showing Super and
Normal Regions after SN-transitions in External Fields

Figure 6 – Post-Draw Annealing Schedule. Sample Numbers and Sequencing are Tabulated as a Function of Time at Temperature

Annealing Time (Minutes)	200	250	300	350	400	450	500	550	600	650
3000	10	3	15					8		1
1000		4	13	14				16	12	
300				22	29		9		6	23
100	25			17	19	28	7			
30					26	21	30	20		11
10	2	18	24			27			5	

Annealing Temperature (°C)

17
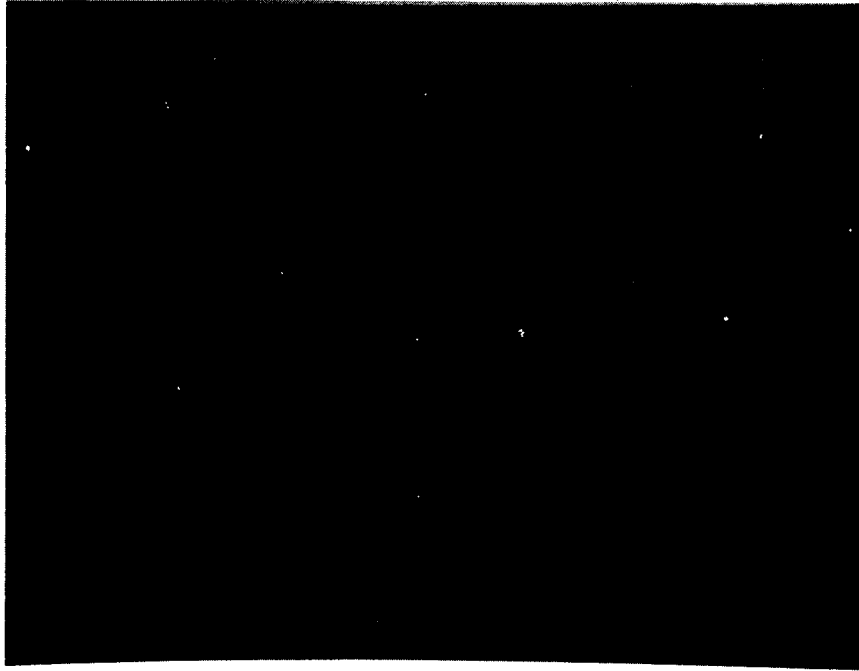
Figure 7 - Characteristic Microstructure of Ti-22 a/o Nb
Cold-swaged to 25-mil, Annealed Two Hours @
800°C and Oil Quenched. Hardness - 184 KHN

250X
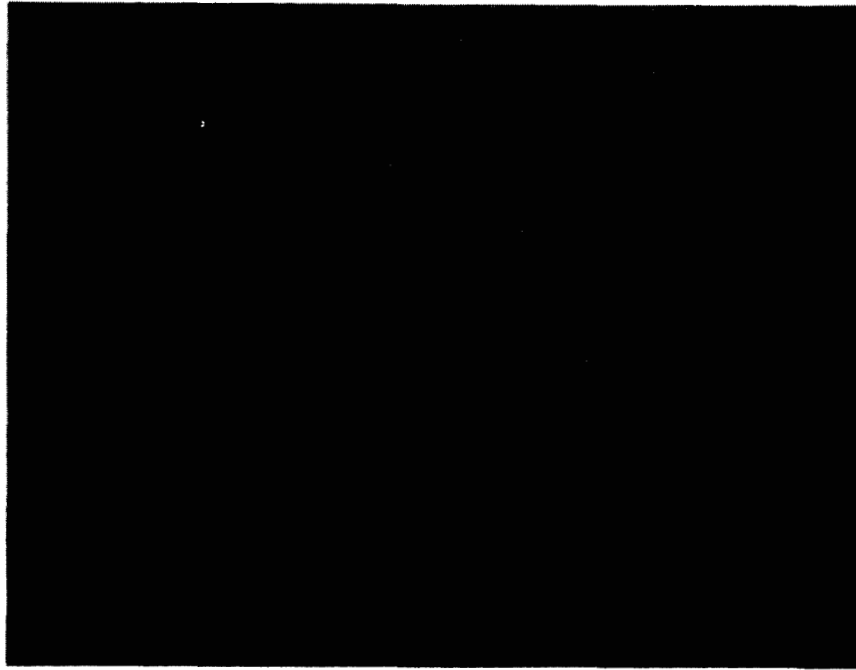
Figure 8a - Characteristic Microstructure of Ti-22 a/o Nb
Cold-swaged to 25-mil, Annealed Four Hours @
550°C and Oil Quenched, and Cold-Drawn to 10-mil
Diameter.   Hardness - 260 KHN.   750X
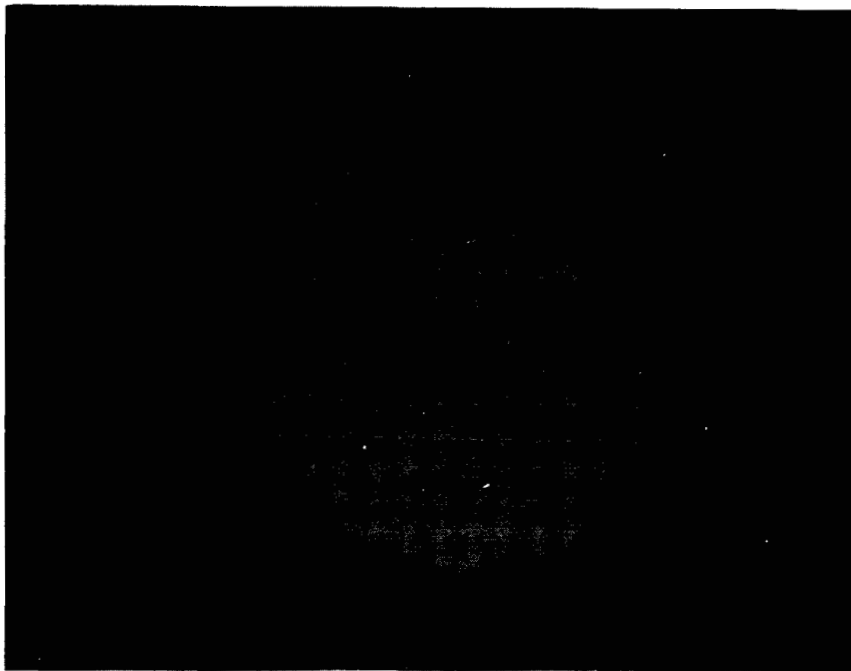
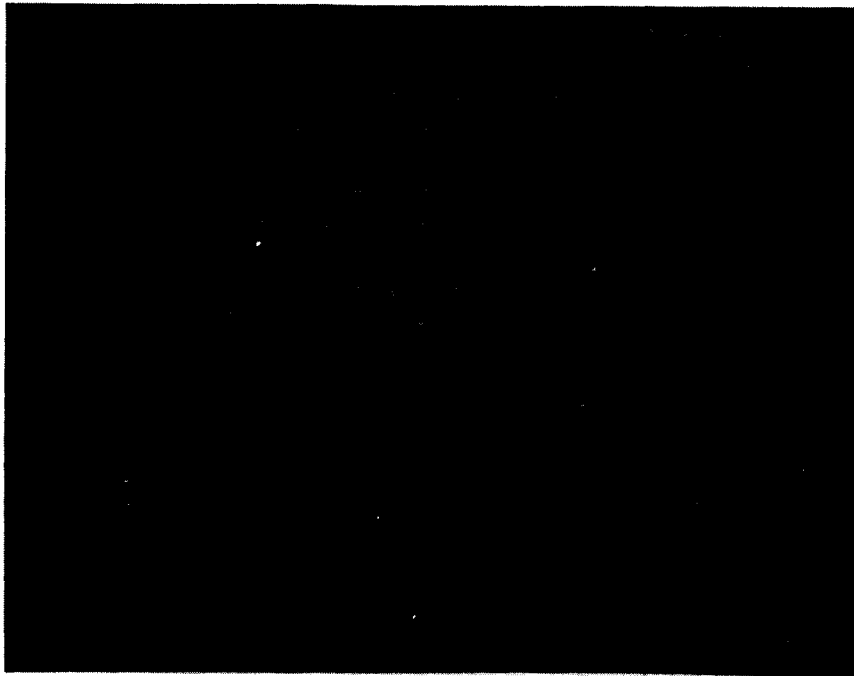Figure 8b - Cross-section of 10-mil Wire shown in 3a.   750X

Figure 9a – Characteristic Microstructure of Ti-22 a/o Nb
Cold-swaged to 25-mil, Annealed Four Hours @
550°C and Oil Quenched, Cold-drawn to 16-mil,
Annealed Two Hours @ 800°C and Oil Quenched,
and Subsequently Cold-drawn to 10-mil Diameter.
Hardness - 290 KHN.   750X
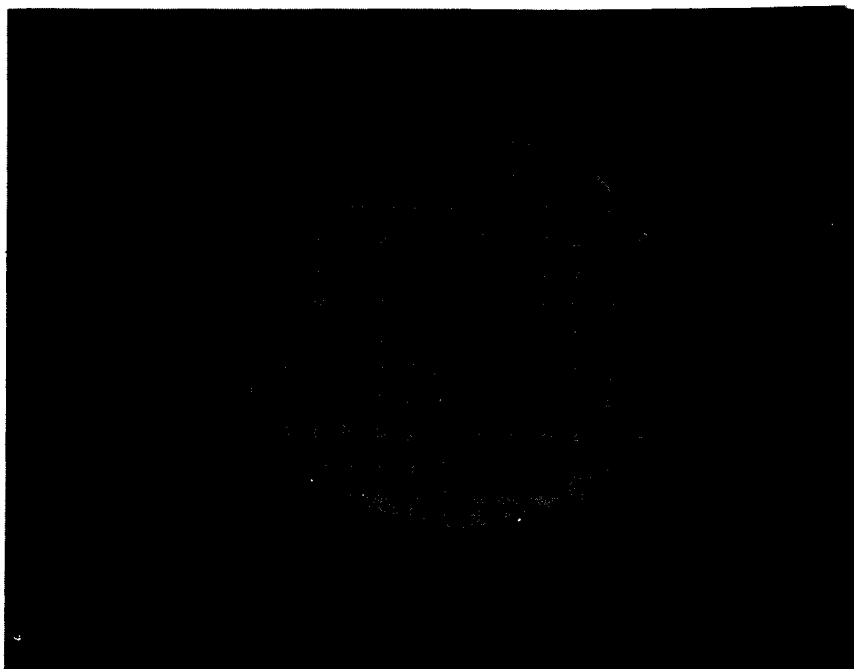
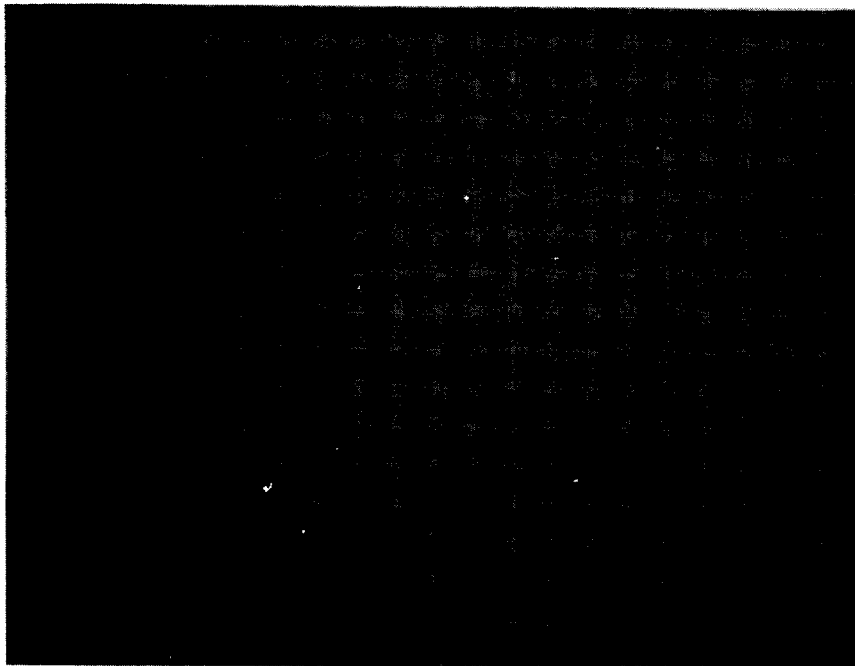Figure 9b – Cross-section of 10-mil Wire shown in 4a. 250X

Figure 10 Characteristic Microstructure Resulting from a
Post-draw Anneal* of 1560 Minutes @ 650°C
(Sample No. 1) Hardness 216 KHN.   750X

Figure 11· Characteristic Microstructure Resulting from a
Post-draw Anneal* of 10 Minutes @ 200°C
(Sample No. 2) Hardness 241 KHN.   750X

*Prior to the post-draw anneals described, the materials in
Figures 6-12 had the following mechanical-thermal history:
1) Cold-swage to 25-mil diameter; 2) four-hour anneal @ 550°C
and oil quench; 3) cold-draw to 16 mils; 4) two-hour anneal @
800°C and oil quench; 5) cold-draw to 10 mil diameter.
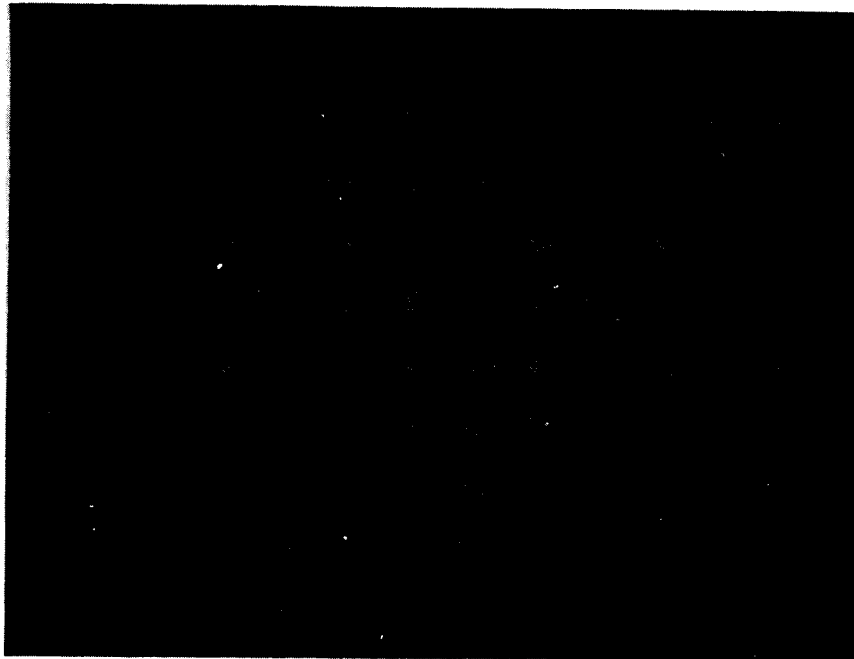
Figure 12   Characteristic Microstructure Resulting from a
            Post-draw Anneal of 3000 Minutes @ 250°C
            (Sample No. 3)   Hardness 480 KHN.   750X

Figure 13 Characteristic Microstructure Resulting from a
            Post-draw Anneal of 1000 Minutes @ 250°C
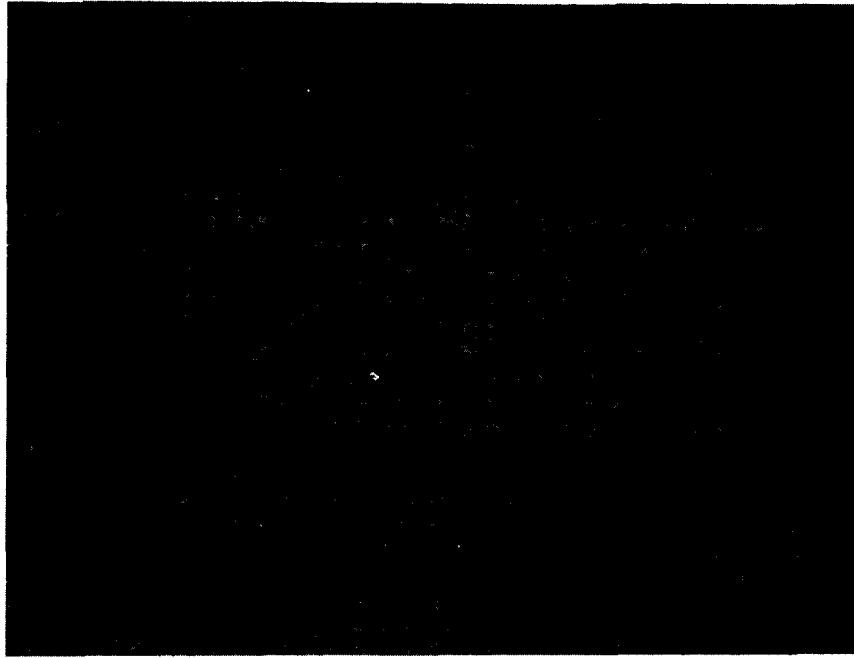   (Sample No. 4)   Hardness 426 KHN.   750X

22

Figure 14 . Characteristic Microstructure Resulting from a
Post-draw Anneal of 10 Minutes @ 600°C
(Sample No. 5)   Hardness 226 KHN.   750X

Figure 15 - Characteristic Microstructure Resulting from a
Post-draw Anneal of 300 Minutes @ 600°C
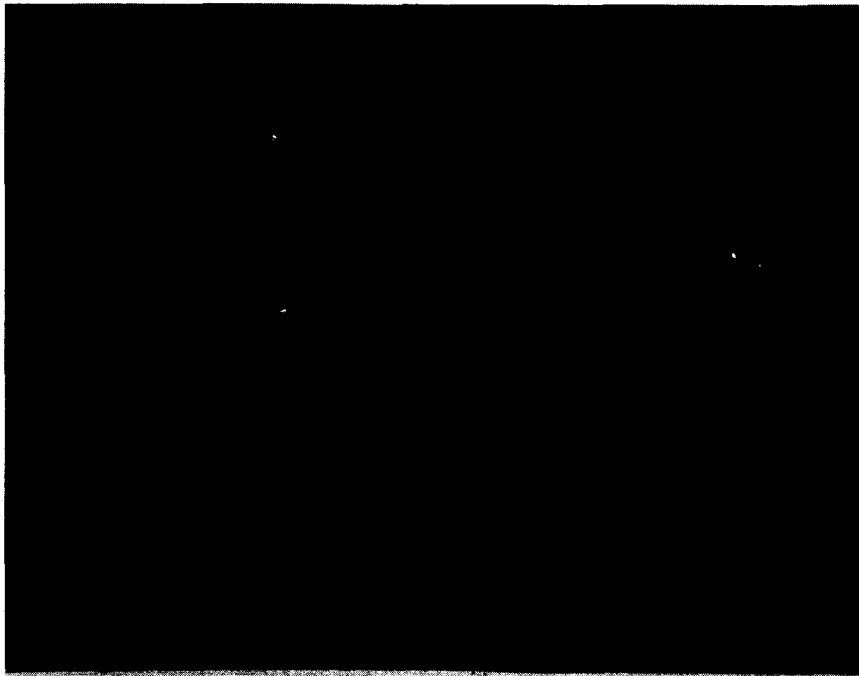(Sample No. 6)   Hardness 236 KHN .   750X

23

Figure 16 - Characteristic Microstructure Resulting from a
Post-draw Anneal of 114 Minutes @ 500°C
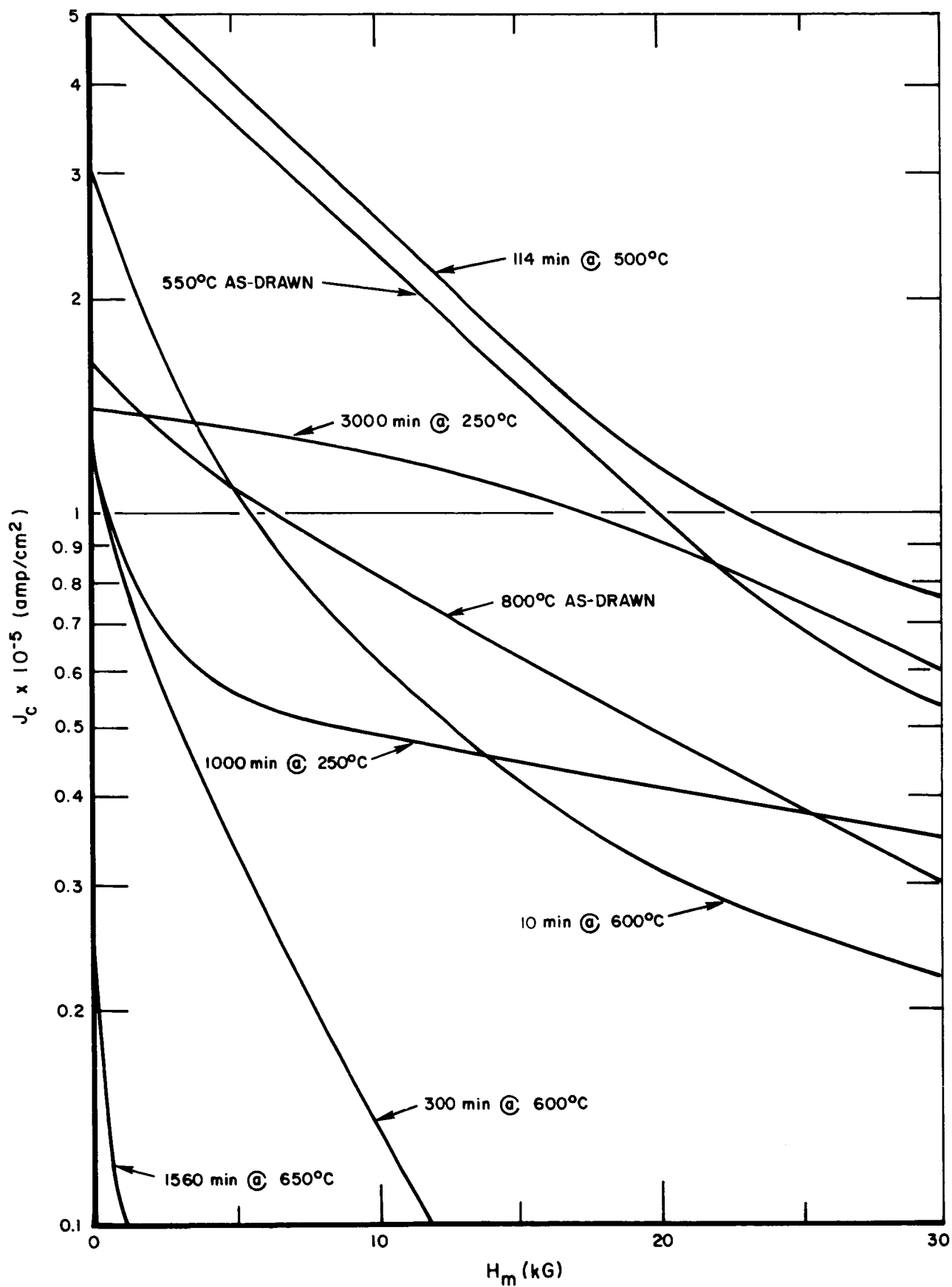(Sample No. 7) Hardness 211 KHN.   750X

Figure 17   Critical Currents in Transverse Applied Fields for 0.010" dia
            Ti-22% Nb Wire after Various Heat Treatments.